

Post-Deposition Induced Conductivity in Pulsed Laser Irradiated Metal Doped Zinc Oxide Films

Lisa J. Wang

Office of Science, Science Undergraduate Laboratory Internship
Program

Correspondence: wangl@carleton.edu

Carleton College, Northfield, Minnesota

Pacific Northwest National Laboratory
Richland, Washington

August 19, 2009

POST-DEPOSITION INDUCED CONDUCTIVITY IN PULSED LASER IRRADIATED METAL DOPED ZINC OXIDE FILMS

Lisa J. Wang (Carleton College, Northfield, Minnesota 55057), Greg J. Exarhos (Pacific Northwest National Laboratory, Richland, WA 99352)

ABSTRACT

The optical and electrical properties of doped solution-deposited and *rf* sputter-deposited thin metal oxide films were investigated following post deposition pulsed laser irradiation. Solution deposited films were annealed at 450 °C. Following the heating regimen, the transparent metal oxide films were subjected to 355 nm pulsed Nd:YAG laser irradiation (4 nsec pulsewidth) at fluences between 5 and 150 mJ/cm². Irradiation times at pulse frequencies of 30 Hz ranged from seconds to tens of minutes. Film densification, index change and a marked increase in conductivity were observed following irradiation in air and under vacuum of Al:ZnO (AZO), Ga:ZnO (GZO), and In:ZnO (IZO) films deposited on silica substrates. Despite the measured increase in conductivity, all films continued to show high transparency on the order of 90% at wavelengths from the band edge well into the near infrared region of the spectrum. Laser energies required for turning on the conductivity of these films varied depending upon the dopant. Irradiations in air yielded resistivity measurements on the order of 16 Ω·cm. Resistivities of films irradiated under vacuum were on the order of 0.1 Ω·cm. The increase in conductivity can be attributed to the formation of oxygen vacancies and subsequent promotion of free carriers into the conduction band. All irradiated films became insulating again after around 24 hours. Oxygen atoms in air became reduced by electrons in the metal conduction band and diffused into vacancies in the lattice. The rate of this reduction process depends on the type of dopant. This work also sheds light on the damage threshold, correlating the optical properties with the presence of free carriers that have been introduced into the conduction band. All films were characterized by means of UV-VIS-NIR transmission spectroscopy, visible and UV Raman spectroscopy and Hall measurements. Analysis of interference fringes in measured transmission spectra allowed film density and refractive index to be evaluated while the Raman measurements showed an increase in LO mode intensity with respect to the TO mode intensity as the films became more conducting. Results of this study are not only important for the continued development of transparent conducting oxide films that find use in photovoltaic cells and solid state lighting modules, but also provide evidence for the role of free carriers in initiating the laser damage process in these wide bandgap metal oxide films.

INTRODUCTION

With awareness to high levels of carbon dioxide emissions and finite fuel resources the increased demand for alternative greener forms of energy, such as solar energy, gives momentum to engineering conductive metal oxide films (TCO films) that are integral components of solar cells and efficient solid state lighting devices. A plethora of technologies and gadgets need to be engineered in order to make the various alternative forms of energy feasible and cost effective. In recent years, solar energy, at the frontier of the alternative energy wildfire, attracted both public attention and a “\$787 billion stimulus package” from the Obama administration, as quoted by the New York Times on February 17, 2009 [1].

Robust transparent conducting oxide (TCO) films enable green energy conversion technologies that can mitigate deleterious environmental effects of coal fired plants. For example, indium tin oxide (ITO) coatings allowed consumers to upgrade their televisions to plasma screens, and liquid crystal displays (LCD) [2]. TCO films are also gaining importance in the emerging area of phototherapeutics, which involves both large scale treatments of skin diseases and stimulated healings of minor skin injuries by LED irradiation at long wavelengths.

Many applications of TCO films require optimal electrical properties while maintaining film transparency, thus, calling for careful control of processing conditions. The optimal parameters can be found through manipulating deposition parameters in the formation of the films, thereby changing the chemical composition, such as the nature and extent of defects in the structure and resident film morphology, including texture,

homogeneity, and crystalline [3]. Both *n*-type and *p*-type wide bandgap semiconductors comprise TCO films. *n*-type conductivity results from an increase of free carriers in the conduction band promoted from energy levels of the dopants in close proximity to the conduction band energy. Conversely, promoting electrons from the valence band into nearby dopant energy levels leads to hole formation in the valence band and concomitant *p*-type conductivity. Thus, while *n*-type conductivity is dependent on the number of electrons in the conduction band, *p*-type conductivity depends on the vacancies in the valence band. Charge carrier mobility also is of critical concern.

One explanation for the conductive nature of TCO semi-conductors is based on a phenomenological theory. For both *p*-type and *n*-type semiconducting oxides with bandgaps greater than 3 eV the key parameters, carrier mobility (μ), effective free carrier mass (m_e), and carrier density (N_e) are important in determining the ability of a specific transparent oxide to acquire conductivity. Medvedeva shows that large free carrier mobility and a small effective free carrier mass are most desirable [4]. Furthermore, the phenomenological theory identifies the necessary parameters for simulating a reflection spectrum of the TCO film and from there the charge mobility can be optimized to give a preferable balance of electrical and optical response. The theory relates these fundamental parameters to the dielectric constant (ϵ) of the material that in turn is used to extract the complex index $\langle \mu \rangle$ and the reflectivity $\langle R \rangle$. For a TCO the extinction coefficient (k) is small, while the refractive index (n) is often near 2 [5].

$$\langle n \rangle^2 = (n + ik)^2 = \epsilon$$

$$R = (n - 1)^2 / (n + 1)^2$$

Doped zinc oxide (ZnO) with a bandgap of 3.3 eV at room temperature is known to be a relatively stable, colorless, and transparent n-type II-VI semiconductor when free carriers are promoted to its conduction band [6]. Zinc oxide films have replaced the more common tin oxide films because they are nontoxic, and more cost effective. When zinc oxide films are appropriately doped, electrons from the oxygen vacancy defect levels are thermally promoted to the conduction band of zinc, upon their release from the material. In this reduced state, the excess oxygen electrons occupy defect levels and are easily excited thermally to the conduction band. The transfer of electrons to zinc's conduction band will create a surplus of free carriers in the conduction band, thus, driving conductivity. Processing conditions are critical to maintaining conductivity without degrading optical response.

The ionic bonds in zinc oxide form a tetrahedral center in the wurtzite crystalline form. Zinc is most similar to aluminum, gallium, and indium in ionic size, this allows for effective lattice substitution of Zn by any of the three dopants.

Imposing rational changes in the deposition process is one area of interest in manufacturing TCO films. ZnO films can be made conductive by modification of deposition parameters and by post deposition processing. There are several different methods of depositing thin films including magnetron sputtering, sol-gel processing, spray pyrolysis, and pulsed laser deposition. Singh et al. induced conductivity in a transparent AZO film by a pulsed laser deposition process in several millitorr of oxygen [7]. Some post deposition techniques to enhance the conductivity of ZnO films involve controlling annealing temperatures, and controlled post deposition laser irradiation.

Radio-frequency magnetron sputtered *n*-type aluminum doped zinc oxide (AZO) films are reported to have resistivities on the order of $7.5 \text{ E-4 } \Omega \cdot \text{cm}$ with optical transmittance over 85%. Somewhat related studies show that film resistivity can be reduced upon pulsed laser irradiation above the bandgap energy. Tsang et al. irradiated sol-gel deposited 2% AZO films annealed at 300 °C at 248 nm. The resistivity of the laser irradiated AZO film ($44(2) \text{ E-3 } \Omega \cdot \text{cm}$) was lower than the resistivity of the baked film ($330(3) \Omega \cdot \text{cm}$), suggesting that laser irradiation may be more effective at inducing conductivity than the conventional processes of baking films in a reducing environment. While the conductivity increased, the optical properties of the AZO films were degraded. The experiment yielded an average transmittance of 86% [8].

This work investigates the possibility to carry out post deposition laser irradiation of solution deposited doped ZnO films (at room temperature) to enhance film conductivity while maintaining high optical transparency. All ZnO films investigated here containing 2% Al, Ga, or In have been prepared by solution or sputter deposition approaches. The films are subjected to variable laser fluences above the bandgap energy in order to determine the optical conditions that enhance the conductivity without damaging the film and decreasing light transmission.

Treated films were expected to become conductive and remain transparent owing to oxygen loss by the irradiation procedure and subsequent formation of donor defect levels from which electrons could be promoted to the conduction band. These electrons then become free carriers and induce conductivity into the film. A decrease in resistivity can then be characterized in Hall measurements as well as from ratios of the intensities of

the LO and TO mode peak intensities in measured Raman spectra and band edge shifts in the transmittance spectra owing to the Moss-Burstein effect [9].

MATERIALS AND METHODS

Precursor Deposition Solutions

All precursor solutions for the deposition of doped zinc oxide films consisted of 3.14 grams of zinc acetylacetonate hydrate powder and 2% of metal nitrate in 10-20 mL of absolute ethyl alcohol with a 1-1.5 mL acetic acid addition to mitigate oxide precipitation. The solubility of zinc acetylacetonate in ethyl alcohol depends on the temperature of the solvent prior to the addition of the powder. Zinc acetylacetonate dissolved completely only in heated (60-70 °C) ethyl alcohol after the addition of 1-1.5 mL acetic acid to form a clear yellow solution. The selected dopant was then added to the clear heated solution of zinc acetylacetonate. Once cooled to room temperature, the solution consistently had a lifetime of approximately one hour before zinc oxide started to precipitate. If continually heated, the precursor solution remained clear for a longer period of time, but then slowly started becoming opaque.

Solution Deposition of ZnO Films

One inch diameter quartz substrates were cleaned prior to film deposition. Organics were evaporated from the quartz substrates by heating the substrates in air to 450 °C for 5-10 min. After the substrates were cleaned, they were affixed to the vacuum chuck of a Specialty Coating Systems P6204-A spin coater.

Spin coating parameters were varied in order to obtain a relatively homogenous and smooth film. Ten drops of precursor solution were dropped onto the surface of each substrate following filtering through a 10 µm millipore filter. Following many trials, the

films produced by spinning the substrate up to 2500-3200 rpm for a total of 30-50 s of spinning time were most uniform; each single layer had a thickness of about 20 nm.

After film deposition, the substrates were immediately removed from the spin coater and heated on a hot plate at 450 °C for 1-2 min. Coated substrates were then quenched on a steel block to room temperature.

This deposition process with spin speed of 3200 rpm was repeated 25 times using a precursor solution containing 20 mL ethyl alcohol for one AZO film sample, to form a multilayer film with a thickness of 432 nm. All other AZO films consisted of 10 coats with total thicknesses of 200 nm. Several IZO films were prepared with 10 coats of precursor solution: 10 mL ethyl alcohol solution, and spun up to 2500 rpm. *Rf* sputter deposited GZO films prepared previously were 653 nm in thickness [10].

Pulsed Laser Irradiation of ZnO Films in Air

Metal oxide films were first irradiated with 355 nm light using a Q-switched Spectra-Physics Quanta Ray GCR-5 Pulsed Nd: YAG Laser with a 3rd harmonic generation from a temperature stabilized NLO crystal. Pulse frequencies of 30 Hz with a 4 ns pulse width were used. 432 nm AZO films were irradiated for 50 min at 20 mJ/pulse, 100-200 nm IZO films were irradiated for 50 min at 8 mJ/pulse, and, 600 nm sputter deposited GZO films were irradiated for 50 min at 20 mJ/pulse and then for 30 min at 50 mJ/pulse. All irradiations were repeated multiple times to optimize irradiation conditions and to ensure the reproducibility of the tests.

The beam exiting the laser is comprised of three wavelengths; (1) fundamental of 1064 nm; (2) half the harmonic frequency of 532; and (3), one-third the harmonic frequency of 355 nm. The light was passed through a 60° spectroscopic prism as it exited

the laser. The prism bends the UV, visible, and IR wavelengths to different extents, thus, allowing for the isolation of the UV light beam (355 nm). Beam dumps were set up to capture the unwanted 532 nm and 1064 nm light. A high reflector at all wavelengths other than the UV filtered the 355 nm light beam to ensure the purity of the beam. The mirror deflected 87% of 1064 nm, 71% of 532 nm and 54% of 266 nm light. The mirror directed the 355 nm light to a film stage for the irradiation studies. An aperture to control the diameter of the beam was placed in the beam path. The laser power was measured using a Scientech Vector S200 power/energy meter and with a Scientech PHD25 detector calibrated at 2.05 V/J. Measurements were taken prior to film irradiations and following the irradiations (Figure 1).

Sample preparation for post-deposition irradiation involved scribing four quadrants on the film. Each quadrant received a different test with varying conditions and parameters. The laser beam for irradiation fit within each quadrant of the film. The diameter of the laser beam was measured to be .65(5) cm.

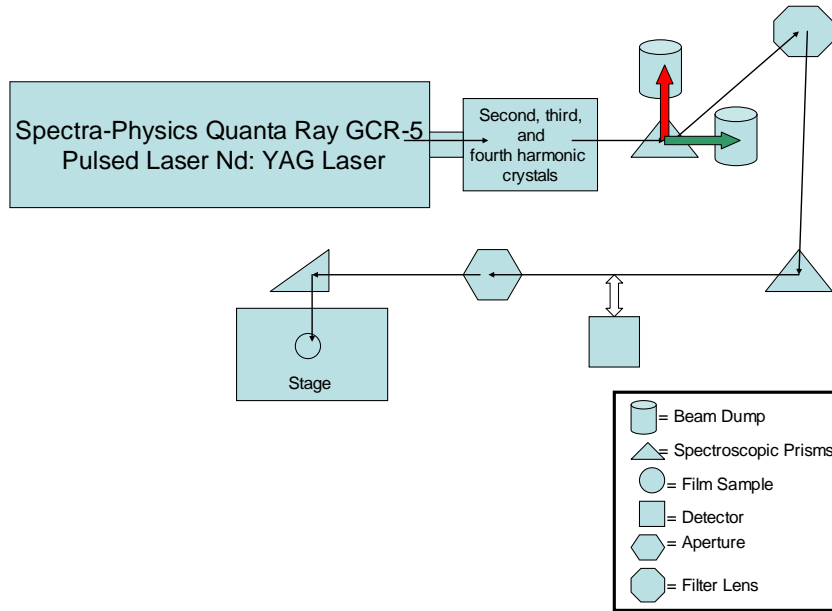


Figure 1. Laser irradiation setup for the 355 nm laser beam post deposition irradiation experiments. Laser beams are indicated by arrows; green and red arrows show IR and visible light trapped in beam dumps while black arrows indicate the path of the 355 nm beam.

The laser fluence (F) is calculated from equation (1).

$$F = \text{Laser Pulse Energy } (P) / \text{Area of Film } (A) \quad (1)$$

Substituting $\pi(d^2/4)$ for A in equation (1),

$$F = P / \pi(d^2/4) \quad (2)$$

A calculation using equation (2) yields 61 mJ/cm^2 for the irradiation of AZO films, 24 mJ/cm^2 in the irradiation of IZO films, and 61 mJ/cm^2 for GZO irradiations. Above 10 mJ/pulse or 30 mJ/cm^2 , IZO films showed surface damage.

The estimated error in the fluence for each irradiation is determined from the partial derivative of equation (2), where the uncertainties in measured pulse energy (δp) and laser footprint diameter (δd) are $\delta p = 10\%$ and $\delta d = 3\%$.

$$\delta f = (4 / \pi d^2) \delta p + \text{abs}[(4P / \pi) * (-2 / d^3) \delta d \quad (3)$$

For all AZO films the error is less than 10%, thus the fluence is 61(5) mJ/cm².

Calculation for the error in the fluence of IZO films irradiations are also less than 10%, and the fluence is 24(2) mJ/cm². The error calculation for the fluence of GZO irradiations is identical to that of AZO irradiations. The fluence of a second irradiation of the GZO film samples is 1.5(1)E+2 mJ/cm².

Pulsed Laser Irradiation of ZnO Films under Vacuum

AZO, GZO, and IZO films were also irradiated in the absence of air at 355 nm using a Q-switched Spectra-Physics Quanta Ray GCR-5 Pulsed Nd: YAG Laser. See Figure 1 for laser irradiation setup. Samples were placed on a substrate holder in a Hall system cell with a quartz window. Sealing the cell creates a vacuum chamber, which is evacuated by a turbo molecular pump connected to the cell with taigon tubing. A Baratron power reader was used to read pressure levels. All measurements were carried out at a pressure of 1 mTorr. AZO and GZO films were irradiated at 61(5) mJ/cm² while IZO films were irradiated at 24(2) mJ/cm².

Metal Oxide film Characterization

UV-VIS-NIR transmission spectroscopy was used to characterize films pre-irradiation and post-irradiation for a comparison in the location of the band edge, film thickness, and film optical properties. Blank spectra for all sample quadrants of the films were collected. Another transmittance spectrum was taken after an irradiation of a sample quadrant. The two spectra were analyzed using Tauc plots to detect shifts in the band edge upon irradiation [11]. The transmission spectrum of the substrate and film was divided by the spectrum of the substrate alone to obtain the transmittance and hence the

absorption coefficient (α). Tauc plots ($\alpha^2(\lambda)$ vs. E) were generated using $-\log T = \alpha d$, where $d = 20$ nm. To detect changes in the thickness of the films throughout the irradiation process, fringe data was collected from UV-vis transmittance spectra and analyzed by an algorithm developed for Mathematica^(T).

After irradiation the inelastic Raman scattering of the LO and TO modes of ZnO films were measured with 514 nm excitation. An INNOVA 300C COHERENT laser operating at 0.5 watts was incident on the sample. Film samples were placed on a stage allowing a $z(y,x)z$ back scattering geometry. This arrangement minimizes the substrate scattering intensity and allows the vibrational features of the film to be seen. In this arrangement, only the p -scattering component will be recorded, and because the substrate scattering is principally s -type, film substrate scattering with respect to that of the film is minimized. The s -scattering from the polycrystalline film has lost its polarization dependence due to the rough surface.

Peak intensity ratios for ZnO arising from the LO and TO modes were compared from measured Raman spectra following baseline correction and peak fitting using GRAMS software. Both the blank samples and the irradiated samples were acquired from an accumulation of 23 scans each with an exposure time of 150 sec. The peaks for the quartz substrate were subtracted from the spectra of each sample. The corrected spectra were fitted by a Lorentzian function to determine intensity values for the TO and LO peaks.

Film Resistivity Measurements

Hall measurements were made for each film sample immediately after irradiation (approximately 7 min) using an MMR Technologies MPS-50 programmable power

supply, H-50 Hall, Van der Pauw controller, and a K-20 programmable temperature controller. All measurements were taken and recorded by a Hall and Van der Pauw System 4.0 using a current of 8.22×10^{-6} A, temperature of 296.06 K, 30 K/min temperature ramp rate, field strength of -3000-3000 G, sensitivity of 0.01 V/kG, and field ramp constant of 100. Film samples were transported from the Nd: YAG laser to the Hall system cell. Four-point measurements were taken and resistivities of all measurements for single films were within 10% of each other. The resistivity, density, and charge mobility values were obtained post-irradiation.

RESULTS

Electrical and Optical Properties of Irradiated ZnO Films

Following laser irradiation for 30 min at fluences of 61(5), 61(5), and 24(2) mJ/cm^2 respectively, AZO, GZO, and IZO films became conductive with resistivities of 15-19 $\Omega \cdot \text{cm}$ while maintaining excellent optical transparency. All post-irradiated films transmitted ~90% of the incident light. No visible change occurred to the AZO film after irradiation; however, subtle change in appearance could be detected within the laser beam footprint for both the GZO and IZO films. Different fluences were required to induce and optimize conductivity in AZO, GZO, and IZO films; IZO films became conductive at a lower fluence, while the fluence needed to invoke conductivity in GZO and AZO films were comparable. However, AZO films became conductive at a marginally lower fluence than seen for GZO films. Film resistivity increased with time immediately after irradiation. The largest increase in resistivity occurred within the first ten minutes after irradiation. All three films became insulating again, after 24 hours of exposure to

ambient air. This result was confirmed numerous times for many different samples. The effect was reversible and could be repeated successively on the same irradiated footprint of the treated films.

The ZnO films damaged, losing their optical transparency, above a critical fluence. The fluence at which the ZnO films damaged depended on the dopant; AZO films damaged around 80 mJ/cm^2 , GZO films damaged around 150 mJ/cm^2 , and IZO films remained undamaged up to around 33.3 mJ/cm^2 . Some damaged films were conductive, but conductivity was lost when the film was completely ablated. Slightly damaged films became opaque and rough as seen under the microscope.

To ensure a measureable change in electrical properties the films needed to be irradiated for at least 30 minutes. A decrease in resistivity was seen within 1 min of irradiation. After 1 hour of irradiation the films were saturated and no further improvement in conductivity was observed. However, if the films were not allowed to recover, irreversible changes to the sample surface morphology were evident.

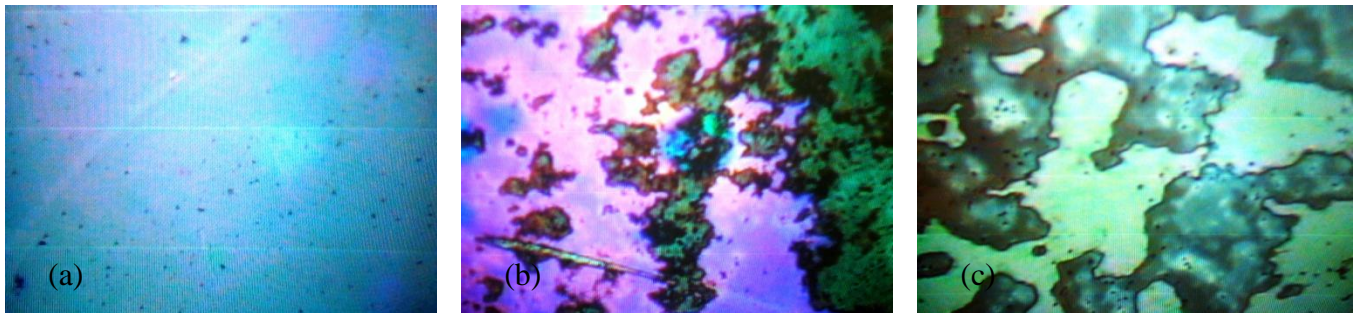


Figure 2. Micrographs of AZO and GZO films; (a) undamaged metal doped ZnO film, (b) damaged AZO film, (c) damaged GZO film.

Blue Shift of the Conduction Band Edge

All transmission spectra of ZnO films: AZO, GZO, and IZO, display a blue wavelength shift in fringe pattern and band edge upon irradiation evident at times up to

24 hours after irradiation. All spectral features show a blue shift as compared with spectra of the unirradiated films. The films begin to recover following equilibration in ambient air for at least 24 hours. Spectra acquired following irradiation show recovery to the original transmission spectra. There does not, however, seem to be a marked change in the maximum transmittance of the irradiated films following equilibration in air.

Transmission spectra of the unirradiated, irradiated, and post irradiated AZO films in Figure 3 display the observed optical changes. The unirradiated AZO film shows the highest %T at nearly 90%. Following recovery, the % transmission is somewhat less. A slight shift of about 1-3 nm, in the band edge also is evident.

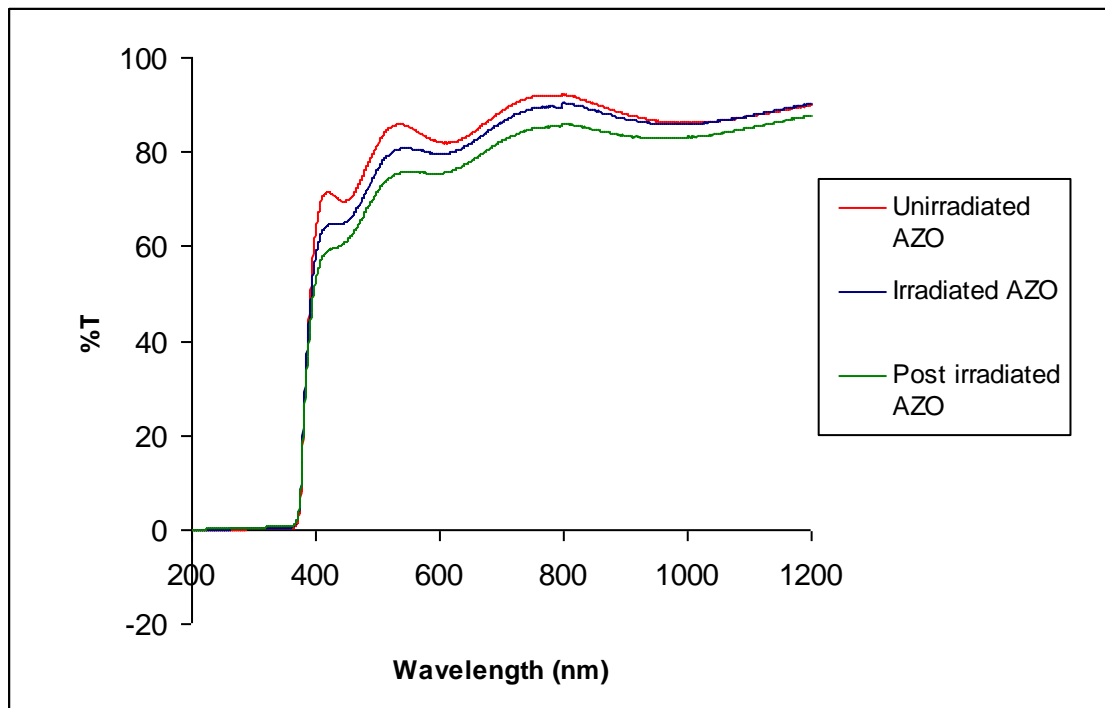


Figure 3. Transmission spectra of a neat, irradiated, and recovered AZO film. Irradiation at 355 nm and 30 Hz for 50 min at a fluence of $61(5) \text{ mJ/cm}^2$.

Similarly, the fringes and band edge of the irradiated GZO film are also slightly blue shifted by a few nanometers (Figure 4) as compared with those of the unirradiated

GZO film. The optical transparency of the irradiated and unirradiated films is comparable at around 90%. The irradiated GZO film seems to have a slightly higher transmission than does the unirradiated GZO film. However, because the GZO film irradiated at 150 mJ/cm^2 for 30 min was damaged, its ability to transmit light was significantly lowered to about 80%. No further shift in the conduction band edge is observed between the GZO films irradiated at 150 mJ/cm^2 and at 61 mJ/cm^2 . The damaged GZO film did not recover and the optical transmission was depressed, however, the conduction band edge of the damaged film shifted back toward the band edge of the unirradiated GZO film. The irradiated GZO film decreased in conductivity after exposure to ambient air for at least 24 hours.

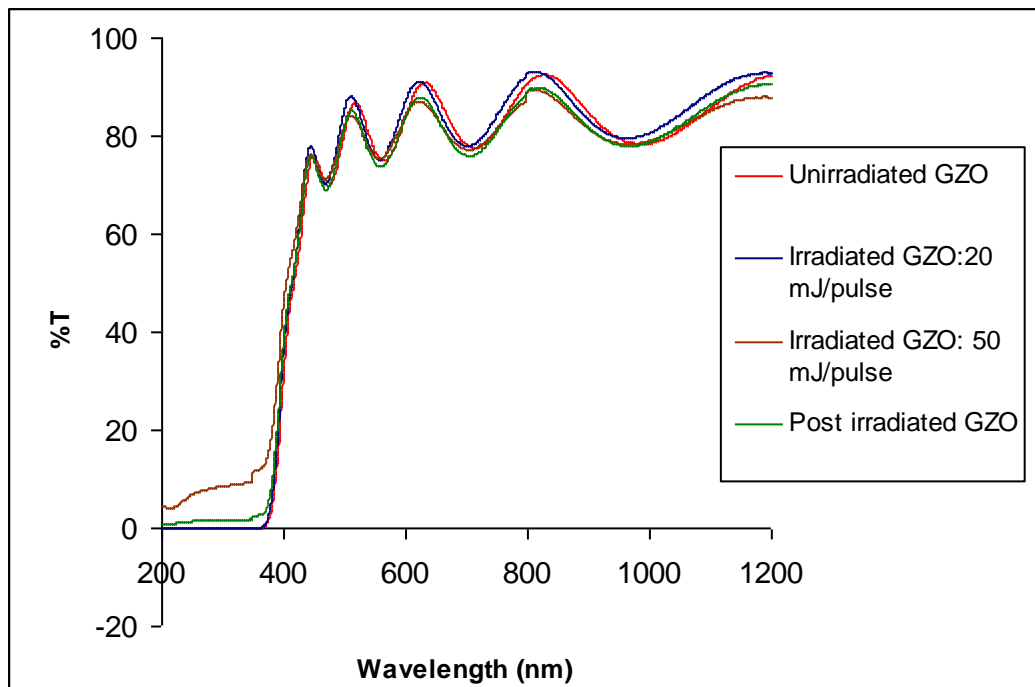


Figure 4. Transmission spectra of GZO films irradiated at $61(5) \text{ mJ/cm}^2$ for 50 min and at $1.5(1)\text{E}+2 \text{ mJ/cm}^2$ for 30 min. Both treatments led to increased conductivity. Irradiation of GZO films at $1.5(1)\text{E}+2 \text{ mJ/cm}^2$ damaged the films, and decreased optical transparency.

A shift in the fringe pattern and conduction band edge of the IZO film was also discernable in Figure 5 from the transmission spectra of the unirradiated, irradiated, and post irradiated films. The measured optical transmittance of the three film samples is similar at around 90%. The band edge of the irradiated IZO film shifted a few nanometers towards the UV and then shifted back to the original position after exposure to air for at least 24 hours.

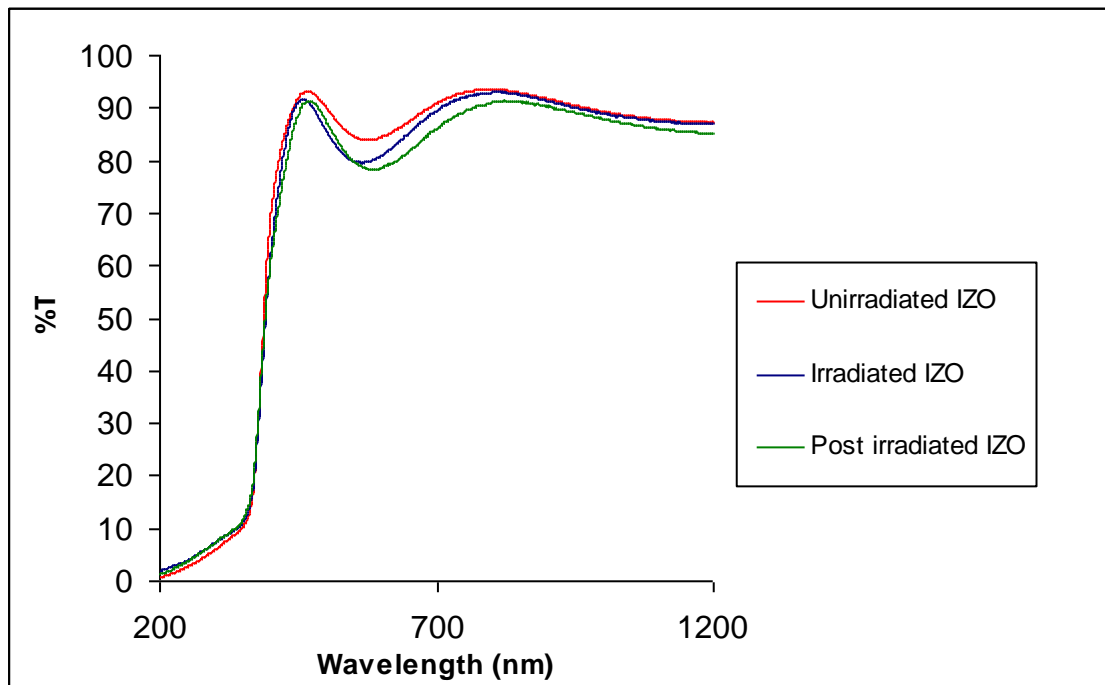


Figure 5. Transmission spectra of unirradiated, irradiated, and post irradiated IZO films. IZO films irradiated at $24(2) \text{ mJ/cm}^2$ showed an increase in conductivity and a blue shift in the band edge.

Raman Mode Intensity Changes

There is a noticeable increase in the ratio of the LO mode peak intensity to the TO mode peak intensity of the irradiated AZO and GZO films annealed at $450 \text{ }^\circ\text{C}$. The LO and TO modes for IZO films were not detectable owing to the poor signal to noise ratio in these very thin films. The allowed transverse TO mode peak at approximately 436 cm^{-1} is attributed to breathing vibrations of oxygen atoms located in tetrahedral coordination

around Zn. The forbidden longitudinal LO mode at approximately 580 cm^{-1} is evident when defects in the ZnO lattice manifest from oxygen vacancies. As sufficient electrons from oxygen are donated to the conduction band upon oxygen release from the lattice, the LO mode intensifies. This observation directly correlates with increased film conductivity.

Raman spectra of unirradiated and irradiated AZO films suggests that the LO mode at 580 cm^{-1} increases with respect to the TO mode at 436 cm^{-1} . The peak at about 1140 cm^{-1} is the first harmonic of the LO mode. The Raman spectrum of the quartz substrate has been subtracted from spectra of the unirradiated and irradiated AZO films shown in Figure 6 to better compare the LO and TO mode intensities.

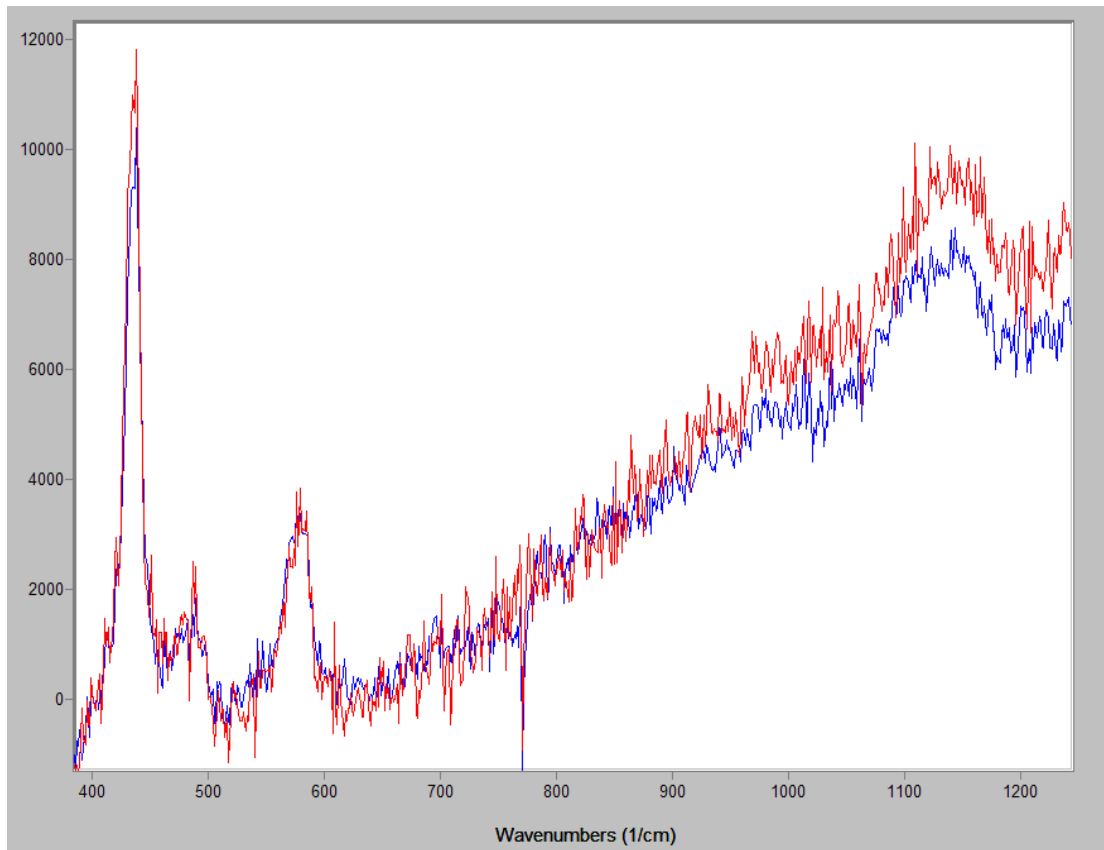


Figure 6. Raman spectra of unirradiated (red) and irradiated (blue) AZO films excited at 488 nm. AZO films were irradiated at $61(5)\text{ mJ/cm}^2$ for 50 min.

The changes of the LO and TO mode peak intensities between the unirradiated and the irradiated GZO films are depicted in Figure 7. Upon irradiation at 355 nm both the LO and TO modes became more prominent. The ratio for the peak intensities of LO mode to TO mode seems largest for the GZO film irradiated at $61(5) \text{ mJ/cm}^2$ for 50 min. At a fluence of $1.5(1)\text{E}+2 \text{ mJ/cm}^2$ for 30 min the GZO film damages and the ratio of peak intensities of the LO mode to the TO mode seems to decrease.

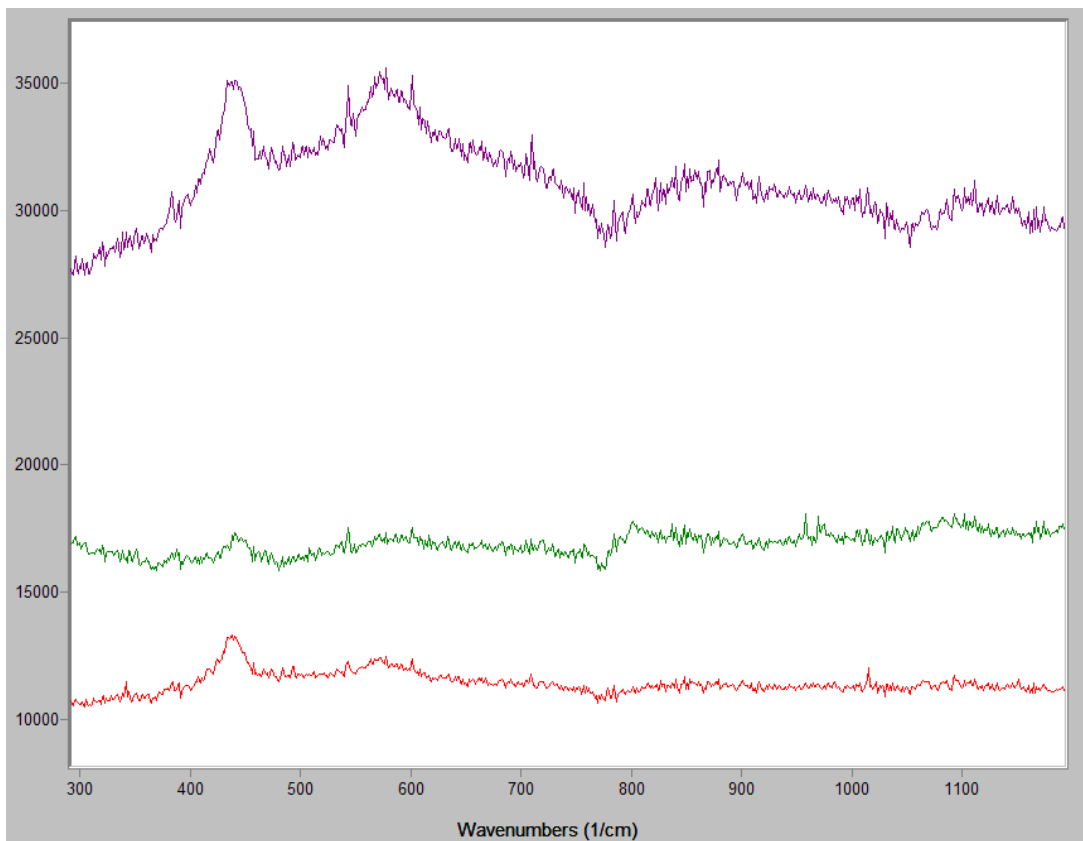


Figure 7. Raman spectra of an unirradiated GZO film (green) and irradiated GZO films. GZO films were irradiated at $61(5) \text{ mJ/cm}^2$ for 50 min (purple) and at $1.5(1)\text{E}+2 \text{ mJ/cm}^2$ for 30 min (red).

Film Resistivity Measurements

Initially, non-conducting, AZO, GZO, and IZO films show decreased resistivity after a 30-50 min irradiation treatment in ambient air at room temperature. Results from Hall measurements appear in Table 1.

Table 1. Hall Measurements of Post Irradiated AZO, GZO, and IZO Films

	AZO	GZO	IZO
Resistivity ($\Omega \cdot \text{cm}$)	17.0	19.2	16.0
Mobility (cm^2/Vs)	-0.126	-17.0	- 8.15
Density (cm^{-3})	-2.92E+18	-1.91E+16	- 4.80E+16
Hall Coeff. (cm^3/Coul)	-2.14	-326	-130
Sheet Number (cm^{-2})	-1.17E+14	-1.15E+12	- 9.60E+11
Sheet Res. (Ω/cm^2)	424733.4	320038.7	798319
Type of Carriers	electrons	electrons	electrons

Post deposition irradiation of ZnO films leads to an increase in conductivity.

Pulsed Laser Irradiation of ZnO Films under Vacuum

Irradiation of AZO, GZO, and IZO films in an evacuated cell (1 milliTorr) markedly enhanced the conductivity of the metal oxide films over that seen in films irradiated in air. Both electron mobility and the carrier density of AZO films increased (Table 1 and Table 2). The electron mobility of the GZO film decreased while its electron density increased. For IZO, both electron mobility and electron density increased.

Table 2. Hall Measurements of Post Irradiated AZO, GZO, and IZO films Under Vacuum

	AZO	GZO	IZO
Resistivity ($\Omega \cdot \text{cm}$)	0.190	0.763	0.141
Mobility (cm^2/Vs)	-0.477	-0.222	-19.0
Density (cm^{-3})	-6.89E+19	-3.69E+19	-2.34E+18
Hall Coeff. (cm^3/Coul)	-9.06E-02	-0.169	-2.67
Sheet Number (cm^{-2})	-2.76E+15	-2.21E+15	-4.68E+13
Sheet Res. (Ω/cm^2)	4744.098	12720.46	7026.374
Type of Carriers	electrons	electrons	electrons

The ZnO films become more conductive when irradiation takes place in the absence of air.

DISCUSSION AND CONCLUSION

It is apparent that solution deposited AZO, GZO, and IZO metal oxide films can be made conductive by post deposition irradiation at wavelength in excess of the ZnO bandgap energy. The studies carried out in this experiment suggest that donor electrons from lattice oxygen and subsequent oxygen vacancies are the key components in lowering resistivity and inducing ZnO film conductivity.

The blue shift in the band edge and changes in the fringe pattern, as observed in UV-vis transmission spectra of the irradiated ZnO films, correlate with the observation of increased conductivity in the films. Tauc plots (α^2 vs. E) of the unirradiated, irradiated, and post irradiated films were constructed based on the UV-vis transmission data. From these plots the bandgap energy of the unirradiated metal doped ZnO films could be calculated; AZO: 3.28 eV, GZO: 3.25 eV, IZO: 3.21 eV. Only marginal shifts were observed in band edge energy between the irradiated and post irradiated films as compared to those of the unirradiated films. This may be a result of the transient nature of the induced conductivity. Electron promotion to shallow levels in the conduction band is the likely explanation.

The increase in intensity of the LO mode peak as compared to the TO mode peak as seen in Raman spectra of the unirradiated and the irradiated AZO and GZO films validates the proposed mechanism that suggests conductivity in ZnO films is attributed to the promotion of oxygen electrons to the conduction band of ZnO. An increase in the

ratio of LO to TO mode peak intensities of the irradiated ZnO films suggests that a redistribution of electrons occurs. Electrons are transferred from oxygen atoms to the metal cation energy levels of the conduction band, while oxygen atoms are released from the lattice. The release of oxygen atoms creates vacancies in the lattice that relax the Raman selection rules allowing increased intensity of the LO mode.

Table 3. Ratios of LO to TO Mode Raman Peak Intensity of AZO and GZO

	Peak Intensity: LO/TO
Unirradiated AZO	0.28
Irradiated AZO	0.34
Unirradiated GZO	0.65
Irradiated GZO	0.80

*AZO and GZO films were irradiated at 61(5) mj/cm² for approximately 50 min.

The irradiated conductive metal doped ZnO films decreased in conductivity proportionally to the amount of time exposed to ambient air after the post deposition irradiations. Approximately 7 min after irradiation, AZO films have a resistivity of 17 Ω·cm, GZO films have a resistivity of 19 Ω·cm, and IZO films have a resistivity of 16 Ω·cm. After 21 min of exposure to ambient air the resistivity of AZO films has increased to 21 Ω·cm. 35 min after laser irradiation of GZO films the resistivity was recorded to be 31 Ω·cm. The resistivity of IZO films 21 min after laser irradiation was 29 Ω·cm.

The increase in resistivity of the ZnO films as they equilibrate in room air is due to re-oxygenation of the lattice. Laser irradiation at 355 nm may not be high enough in energy to promote oxygen donor electrons far enough into the conduction band to prevent recovery to the insulating state. This relaxation process decreases the number of free carriers in the conduction band and, thus, decreases the conductivity. These electrons can then reduce oxygen which diffuses into the lattice thereby restoring the insulating state by

filling the vacancies. This reduction phenomenon continues until all oxygen vacancies are filled causing the films to become completely insulating again.

The rate at which the post deposition laser irradiated metal doped ZnO films increase in resistivity depends upon the ionic sizes of the metal dopant. IZO films recover rapidly and AZO films are somewhat retarded at increasing in resistivity after the irradiation treatment. Figure 8 presents recovery rate data for the increase in resistivity of the irradiated AZO, GZO, and IZO films. The rates for the increase in resistivity of AZO, GZO, and IZO films are $0.30 \Omega \cdot \text{cm}$, $0.40 \Omega \cdot \text{cm}$, and $0.91 \Omega \cdot \text{cm}$ respectively.

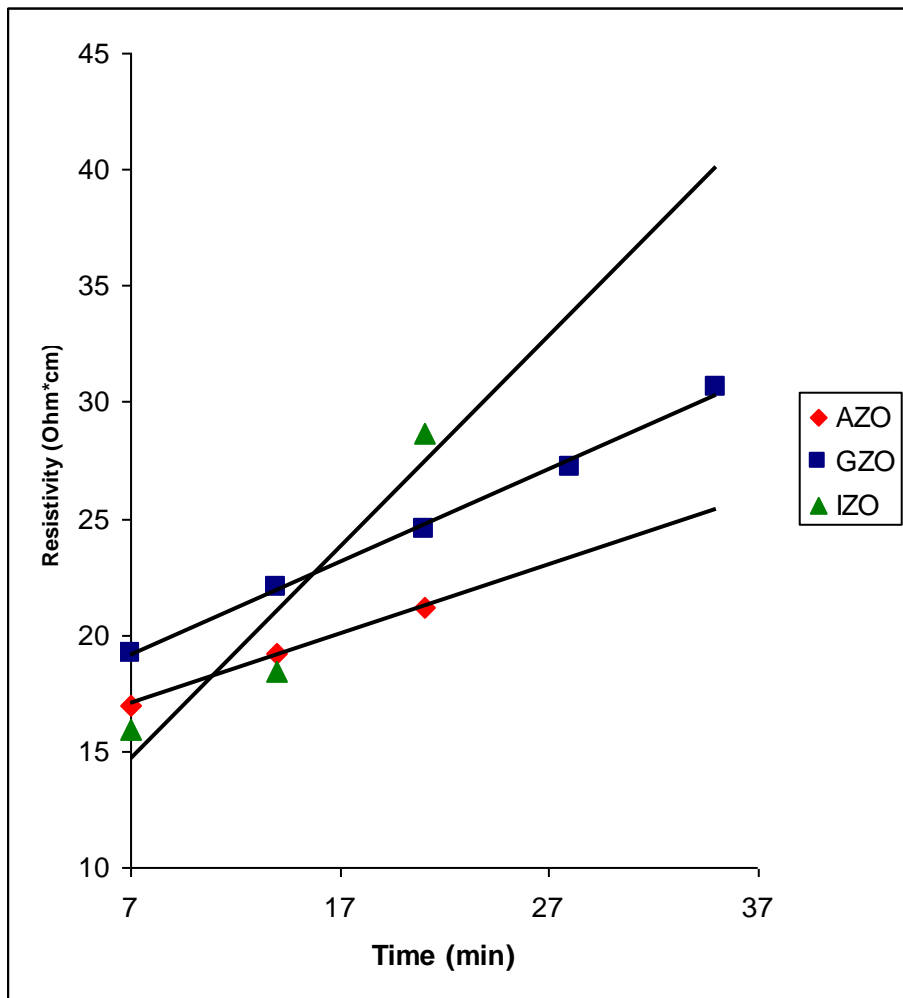


Figure 8. Resistivity vs. time of AZO, GZO, and IZO films.

Because the decrease in conductivity is related to oxygen reduction and re-assimilation into the lattice it follows that the rate for the increase in resistivity also is indicative of the rate at which oxygen fills the vacancy holes in the lattice. A higher rate represents a lattice in which oxygen can more easily diffuse, while a smaller rate is indicative of a lattice that restricts oxygen diffusion and concomitant reduction. Thus, oxygen atoms are more able to enter a more-expanded lattice. The spacing between the Zn atoms and metal dopant atoms are dependent on the strength of the ionic attraction between the atoms. A stronger ionic attraction results in a more compressed lattice, leaving less space for oxygen atoms to insert into the lattice. Thus, a strong ionic interaction between the metal dopant atoms and the oxygen atoms mitigates this process.

Smaller metal dopants, such as aluminum create stronger interactions with oxygen atoms in the lattice because their nuclei are less shielded and there is more positive charge contributed by the nucleus to the ionic bonding with Zn atoms. Also, because the smaller metal dopant atoms have a lower number of electrons, there is less electron repulsion between the metal dopant atoms and the oxygen atoms, thus; the bond between dopant atom and the oxygen atoms is shorter. The shorter ionic bond between the dopant and the oxygen atoms is more apt at preventing oxygen atom ingress into the lattice.

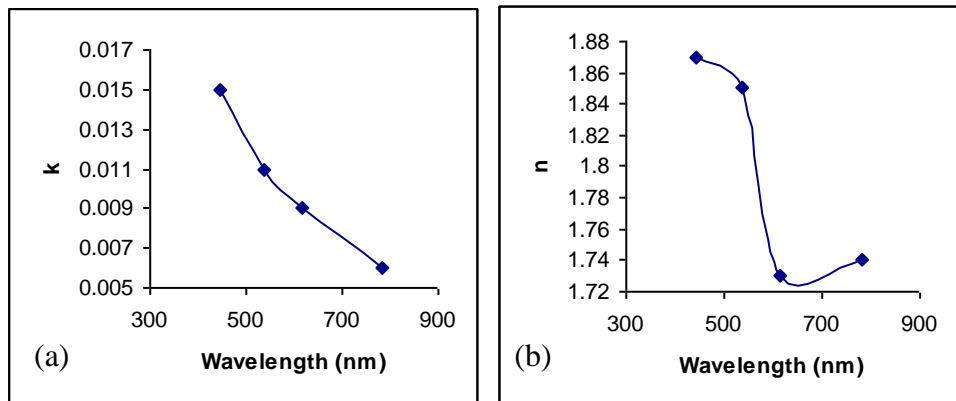
Thus, it is not surprising that, of all three metal doped ZnO films, AZO films have the lowest rate for film lattice re-oxygenation. Aluminum, with an ionic radius of 72 pm and an electron configuration of $[\text{Ne}]3s^22p^1$, has the smallest ionic radius of the three dopants, and has its valence electron in the 2p electron shell. Thus, the bonds between aluminum atoms and oxygen atoms are the strongest and shortest, leaving less room for oxygen atoms to diffuse into the lattice.

It is also not surprising that GZO films lose their conductivity at a faster rate than do AZO films, and at a slower rate than do IZO films. Gallium's ionic radius is 81 pm, which is larger than that of aluminum, but smaller than that of indium (104 pm). Furthermore, the electron configuration of gallium is $[\text{Ar}]4s^23d^{10}4p^1$, suggesting that the nucleus of gallium is more shielded. Because of their larger ionic size, gallium atoms, as compared to aluminum atoms, are associated with weaker and longer ionic bonds with oxygen atoms. The weaker and longer ionic bond allows for a higher diffusion rate.

As expected, IZO films have a significantly higher re-oxygenation rate. Indium atoms are significantly larger in ionic size than both aluminum and gallium atoms. The ionic radius of indium is 104 pm and the electron configuration of indium is $[\text{Kr}]5s^24d^{10}5p^1$, suggesting that the nucleus of indium atoms are more shielded. The ionic interactions between indium dopant atoms and the oxygen atoms are the weakest and the bonds are the longest, making it easiest for oxygen atoms to enter a ZnO lattice doped with indium.

The lowered resistivity of irradiated AZO, GZO, and IZO films under vacuum further supports the crucial role that oxygen plays in donating free carriers to the conduction band of the doped ZnO films. Oxygen was simultaneously pumped out of the cell while the films were irradiated thus creating an oxygen free environment. Vacancies created in the film during irradiation were not being re-oxygenated throughout the irradiation process. In the absence of oxygen the promoted free carriers were more likely to remain in the defect and conduction band energy levels. Once exposed to air, the films started becoming more resistive as oxygen atoms began entering the lattice.

In addition to a change in the electrical properties, the irradiated metal doped ZnO films also changed physically and optically. All metal doped ZnO films compacted upon irradiation, but then relaxed to a thickness close to that of the unirradiated film. The thickness of unirradiated AZO films is 432 nm; the thickness of irradiated AZO films is 349 nm; and, the thickness of AZO films 24 hours after irradiation is 427 nm. The refractive index of the irradiated AZO films increased as compared to that of the unirradiated AZO films and compared to that of the AZO films after exposure to air for 24 hours. There is no significant change in the extinction coefficient between the unirradiated and irradiated AZO films, as both follow a decreasing trend from short to long wavelengths. Similar trends were seen in the optical and physical properties of GZO and IZO films. The correlation between the laser irradiated induction of conductivity and the observed optical and physical parameters could shed light on the laser damage threshold of these metal doped oxide films.



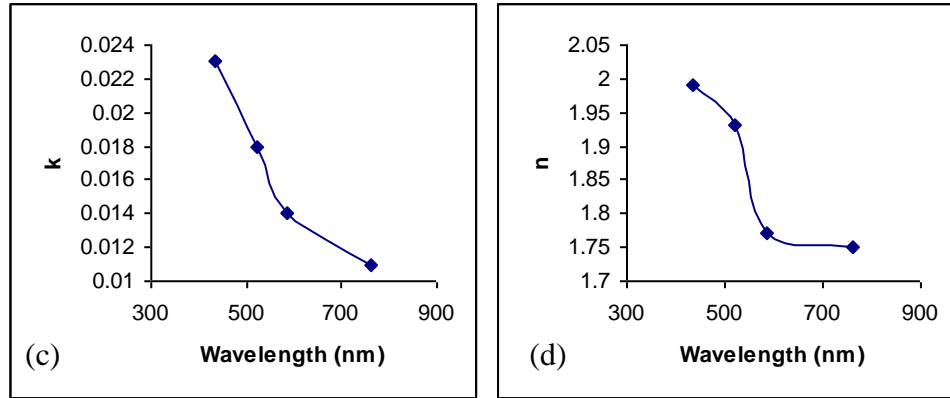


Figure 9. Refractive index and extinction coefficient of AZO films irradiated in air: (a) extinction coefficient vs. wavelength of unirradiated AZO film (b) refractive index vs. wavelength of unirradiated AZO film (c) extinction coefficient vs. wavelength of irradiated AZO film (d) refractive index vs. wavelength of irradiated AZO film

While irradiation of metal oxide doped ZnO films in air at room temperature produced conductive films with 16-19 $\Omega \cdot \text{cm}$ resistivity, irradiation of these films in a reducing environment (CO) at room temperature produced films that were more conductive, with resistivities of 1-4 $\Omega \cdot \text{cm}$, and films irradiated under vacuum at room temperature produced conductive films with the lowest resistivity of about 0.1 $\Omega \cdot \text{cm}$. Laser irradiation at wavelengths close to that of the exciton band of ZnO created oxygen vacancies in the ZnO film lattice, promoting those oxygen electrons into the metal defect and ZnO conduction band energy levels. In room air, there is an excess of oxygen atoms, which are able to enter the lattice filling the oxygen vacancies. Thus, the oxygen atoms that have entered the lattice can relax and deplete free carriers from the conduction band of ZnO and thereby decrease the effects of the initial excitation of those electrons into the conduction band. The conductivity is subsequently lowered. However, under vacuum, excess oxygen is removed from the film and the film becomes oxygen deficient. The

resulting oxygen deficient film has a greater conductivity, owing to a higher free carrier density.

A preliminary experiment involving the irradiation of an AZO film in a cell purged with carbon monoxide, a reducing gas, at 1 atm in room temperature was carried out to verify the importance of oxygen as the key contributor to the induction of conductivity of the metal doped ZnO films. Irradiations were performed under the same conditions as in previous studies described in this paper. The resulting film became more conductive than films irradiated in room air, but had a higher resistivity than films irradiated under vacuum. Further studies investigating the irradiation of the metal doped ZnO films in reducing environments and as a function of temperature would provide valuable detail into the mechanism for transforming insulating metal doped ZnO films into conductive TCO films, and for the role of oxygen in lowering the resistivity of the films and in influencing the damage threshold.

ACKNOWLEDGEMENTS

This research has been supported by the Materials Sciences and Engineering Division of Basic Energy Sciences through the Department of Energy Office of Science. Chuck Windisch assisted in the characterization process of the metal doped ZnO films. Rf sputtered GZO film sample was provided by Pete Martin. Studies were carried out in the Physical Sciences Laboratory at the Department of Energy located at the Pacific Northwest National Laboratory. Battelle Memorial Institute operates PNNL for the U.S. Department of Energy under contract No. DE-AC06-76RLO 1830.

REFERENCES

- [1] K. Galbraith. "Obama Signs Stimulus Packed with Clean Energy Provisions." The New York Times 17 February 2009:
<http://greeninc.blogs.nytimes.com/2009/02/17/obama-signs-stimulus-packed-with-clean-energy-provisions/>.
- [2] F. Zhu. Transparent Electrode for OLEDs. In *Organic Light-Emitting Materials and Devices*; Z. Li, H. Meng Eds.; CRC Taylor and Francis: New York; Chapter 6.
- [3] G. J. Exarhos, and T. Dennis, *Laser-Induced Damage in Optical Materials*, SPIE 2966: 307-314 (1997).
- [4] J. E. Medvedeva, *European Physics Letters* 78: 57004 (2007).
- [5] G. J. Exarhos, and X. Zhou, *Thin Solid Films* 515: 7025-7052 (2007).
- [6] W.M. Tsang, F.L. Wong, M.K. Fung, J.C. Chang, C.S. Lee, and S.T. Lee, *Thin Solid Films* 517: 891-895 (2008).
- [7] A. V. Singh, and R. M. Mehra, N. Buthrath, A. Wakahara, and A. Yoshida, *J. Appl. Phys* 90: 5661-5665 (2001).
- [8] W.M. Tsang, F.L. Wong, M.K. Fung, J.C. Chang, C.S. Lee, and S.T. Lee, *Thin Solid Films* 517: 891-895 (2008).
- [9] G. J. Exarhos, Engineering Performance in TCO Films for Energy Applications, 1-14 (2009).
- [10] G. J. Exarhos, Engineering Performance in TCO Films for Energy Applications, 1-14 (2009).
- [11] Park, T. Ikegami, and K. Ebihara, *Jpn. J. Appl. Phys.* 44: 8027-8031 (2005).